

PROCEEDINGS OF SPIE

SPIEDigitalLibrary.org/conference-proceedings-of-spie

Nano-cone optical fiber array sensors for MiRNA profiling

Yunshan Wang, Satyajyoti Senapati, Paul Stoddart,
Scott Howard, Hsueh-Chia Chang

Yunshan Wang, Satyajyoti Senapati, Paul Stoddart, Scott Howard, Hsueh-Chia Chang, "Nano-cone optical fiber array sensors for MiRNA profiling," Proc. SPIE 8812, Biosensing and Nanomedicine VI, 88120Q (11 September 2013); doi: 10.1117/12.2023727

SPIE.

Event: SPIE NanoScience + Engineering, 2013, San Diego, California, United States

Nano-Cone Optical Fiber Array Sensors for MiRNA Profiling

Yunshan Wang^a, Satyajyoti Senapati^a, Paul Stoddart^b, Scott Howard^c, Hsueh-Chia Chang^{a*}

^aDept. of Chemical and Biomolecular Engineering, Univ. of Notre Dame, Notre Dame, IN USA 46556; ^bDept. of Electrical Engineering, Univ. of Notre Dame, IN USA 46556; ^cFaculty of Engineering & Industrial Sciences, Swinburne University, Melbourne, Hawthorn VIC 3122 Australia

ABSTRACT

Up/down regulation of microRNA panels has been correlated to cardiovascular diseases and cancer. Frequent miRNA profiling at home can hence allow early cancer diagnosis and home-use chronic disease monitoring, thus reducing both mortality rate and healthcare cost. However, lifetime of miRNAs is less than 1 hour without preservation and their concentrations range from pM to mM. Despite rapid progress in the last decade, modern nucleic acid analysis methods still do not allow personalized miRNA profiling---Real-time PCR and DNA micro-array both require elaborate miRNA preservation steps and expensive equipment and nano pore sensors cannot selectively quantify a large panel with a large dynamic range.

We report a novel and low-cost optical fiber sensing platform, which has the potential to profile a panel of miRNA with simple LED light sources and detectors. The individual tips of an optical imaging fiber bundle (mm in diameter with 7000 fiber cores) were etched into cones with 10 nm radius of curvature and coated with Au. FRET (Forster Resonant Energy Transfer) hairpin oligo probes, with the loop complementary to a specific miRNA that can release the hairpin, were functionalized onto the conic tips. Exciting light in the optical fiber waveguide is optimally coupled to surface plasmonics on the gold surface, which then converges to the conic tips with two orders of magnitude enhancement in intensity. Unlike nanoparticle plasmonics, tip plasmonics can be excited over a large band width and hence the plasmonic enhanced fluorescence signal of the FRET reporter is also focused towards the tip--- and is further enhanced with the periodic resonant grid of the fiber array which gives rise to pronounced standing wave interference patterns. Multiplexing is realized by functionalizing different probes onto one fiber bundle using a photoactivation process.

Keywords: Surface Plasmon Resonance, Biosensors, microRNAs, FRET.

1. INTRODUCTION

Abnormal expression of miRNAs has been related to cancers, heart diseases and diabetes [1]. Screening platform based on miRNA profiling is very important for early diagnosis and therapies of diseases. However, short life time and low expression level of miRNAs in early stage of diseases pose challenges for accurate miRNA profiling. Real-time PCR and miRNA microarray have been used to profile miRNAs on a large scale, but they both have disadvantages. Real-time PCR can quantify low amount of miRNAs, but can only detect one target at one time, making it impossible to profile a large number of target miRNAs. DNA microarray can detect thousands of molecules but is unable to detect low concentration miRNAs, which take tens of hours to diffuse to the oligo, probes. There is some recent progress based on using naopores (ref paper from Missouri) for miRNA profiling but the ion current signatures are not sufficient selective to differentiate different miRNAs .

Several label-free nucleic acid sensing technologies have been intensively studied in the last decade. Electrochemical sensors have good detection sensitivity, but suffer from signal instability [2 , 3]. Capacitance, conductance and field-effect transistor (FET) electrode sensors have a detection limit higher than nano-molar, which translates into 10^8 to 10^9 copies of miRNA, too high for miRNA detection. Optical sensors have demonstrated excellent sensitivity down to single molecule level; however, the expenses remain high. Surface Plasmon Resonance (SPR) enhanced optical sensors significantly reduced the need for expensive lasers and detectors, thus making the entire platform portable and less costly. SPR is free electron oscillation coupled with electromagnetic (EM) wave that

exponentially decays away from the metal surface [4]. Therefore, SPR sensors are only sensitive to molecule docking events near the surface of metallic structures, making it insensitive to bulk debris.

Among all nanostructures, nano-cone with sharp curvature sustains the highest field enhancement factor. We studied theoretically the field enhancement for metallic nanocones [4] and obtained optimal conditions to excite SPR on cones. We have also designed experimentally a novel and low-cost optical fiber sensing platform, which has the potential to profile a panel of miRNA with lower cost than traditional methods. SPR on nano-cones dramatically enhanced fluorescent signal upon hybridization of target miRNAs, thus improving detection limit. Multiplexing is realized by taking advantages of thousands of pixels in each fiber bundle.

THEORY

1. 1 Dispersion Relationship

We report theoretically field enhancement by solving Maxwell equations near a perfect metallic cone. Applying the continuity of the field and displacement on the interface and omitting higher order less singular plasmonic modes, a transcendental dispersion relationship [4] is obtained for the dominant eigenvalue ν ,

$$\frac{\varepsilon_m + f(\pi - \alpha, \nu) f_\theta(\alpha, \nu)}{\varepsilon_o f(\alpha, \nu) f_\theta(\pi - \alpha, \nu)} = \frac{\varepsilon_m}{\varepsilon_o} + g(\alpha, \nu) = 0 , \text{ with } f(\theta, \nu) = P_\nu^1(\cos \theta) \sin \theta .$$

Eigen values are related to field enhancement factor and can be computed from the dispersion relationship given the material properties of the metal.

1. 2 Optimal Cone Angle

As field focusing at small cone angles can increase both the field intensity and also the conductive loss, an optimal angle is expected. Figure 1 shows that there exists an optimal angle for maximum field enhancement at different excitation wavelength.

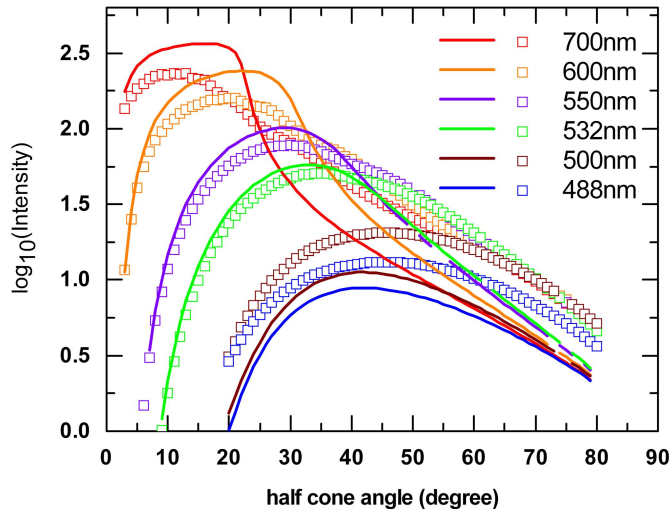


Fig. 1. Comparison of theoretical intensification factor (solid curves) against the literature values of [5] (scattered points) for gold cones of different angles ($R_1=5$ nm, $R_2=300$ nm).

*hchang@nd.edu; phone 1 574 631-5697; fax 1 574 631-8366; nd.edu/~changlab

1.3 Broad Resonance Bandwidth

Due to continuous change of length scale, nano-cone can sustain SPR at a broad range of spectrum. As shown in Fig 2, the entire solar spectrum is excited at small angles. In contrast, the extinction spectrum for a single nanosphere [6] has a bandwidth that is 1/10 of the broadband SPR spectrum for conical nanotips.

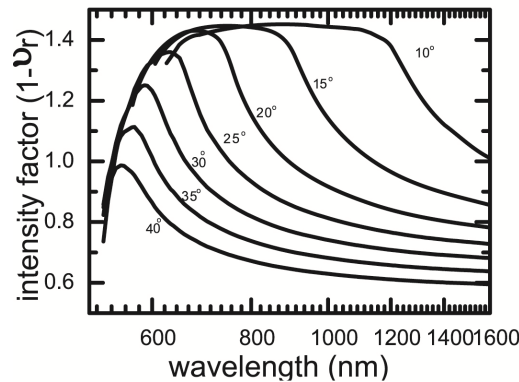


Fig. 2. The intensification exponent for a gold cone with different cone angles and shows the SPR spectrum broadens and exhibits a red shift away from the planar plasmon resonant wavelength.

2. EXPERIMENTS

2.1 Materials

Fused optical fiber bundles (70,000 pixels, FIGH-70-1300N) were purchased from Fujikura. Probe molecules were custom ordered from Integrated DNA Technologies, Inc with fluorescence dye attached (sequence see Table 1). Target microRNAs are mature RNAs for oral cancer marker. Microfluidic channels were made from PDMS (SYLGYRD 184 SILICONE ELASTOMER, Dow Corning). Cover slip slides were purchased from Thermo Scientific, Inc.

Table 1. Sequence of FRET probes and targets.

Probe	5'- /56-FAM/CA GAC AGA ACC CAT GGA ATT CAG TTC TCA CTG TCT GAA AAA A/3ThioMC3-D/ -3'
Target	5'- TGA GAA CTG AAT TCC ATG GGT T -3'

2.2 Fabrication

Imaging Fiber bundle was sectioned into 2 mm length by a wafer dicing saw machine (?Micro Automation Saw Model 1100). The sectioned fibers were then immersed in buffered HF (buffered oxide etch, 10:1, J.T. Baker) for 80 minutes, then thoroughly rinsed under deionized water and dried with compressed nitrogen [7]. Cone angle can be tuned by changing the ratio of HF in buffer solution. A layer of gold film (5 nm) was evaporated onto gold fiber surface (Oerlikon Evaporator, UNIVEX 450 B). SEM image of cone is shown in Figure 3. Microfluidic channel was made by PDMS casting method where a dent with the size of an optical fiber was created above channels and the channel is then plasma treated (Corona?) and bonded with a cover slip.

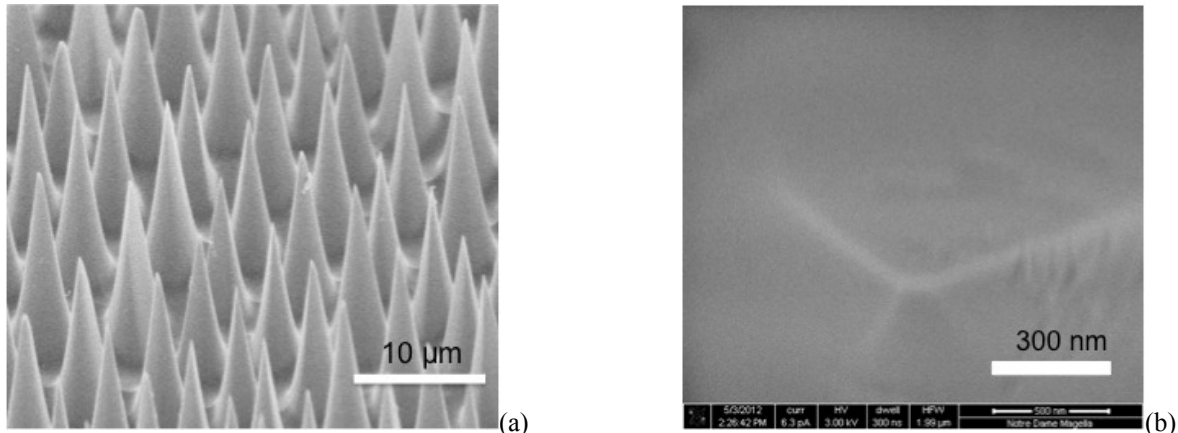


Fig. 3. (a) SEM image of nano-cone array with 10 micro-meters scale bar. (b) SEM image of nano-cone tip with 300 nm scale bar.

2.3 Optical Setup

A PDMS microfluidic channel was placed on top of an inverted fluorescence microscope (IX71, Olympus) where an optical fiber (2 mm) was inserted into a dent created above the microfluidic channel. The cone array was facing downwards toward the microfluidic channel as shown in the schematics.

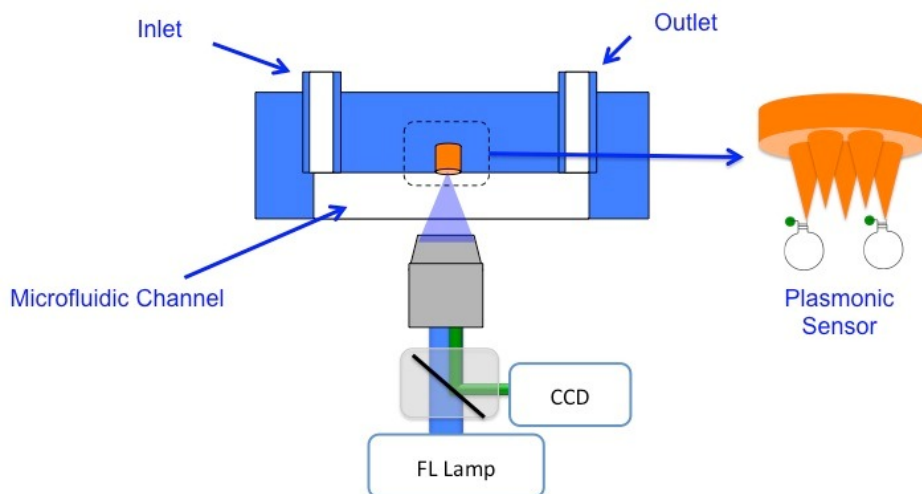


Fig. 4. (a) Schematics show the optical setup for detection of miRNAs. Blue light (488 nm) was shined upon fiber surface and reflected green light (520 nm) was collected by CCD camera (Qimaging ?). Blue part of the device is made of PDMS.

3. RESULTS AND DISCUSSION

Before hybridizing with target miRNAs, fluorescent molecules on hairpin probes are close to metal surface, thus quenched by gold. After hybridization with target miRNAs, hairpin probes open up and push fluorescence away from metal surface, thus releasing fluorescence signal. Fluorescent intensity change after hybridization can be correlated with the concentration of target miRNAs, which can be used to quantify the number of target miRNAs in sample solution. Figure 6 shows a lower detection limit of 1 nM, which corresponds to 1 million copies of miRNAs. Time response curve

shows that fluorescent intensity increases with time and saturates after half an hour for 70 nM concentration. This 30-min assay time is shorter than the typical assay time at 1 nM and is probably due to the enhanced diffusion rate to the cone relative to a flat surface.

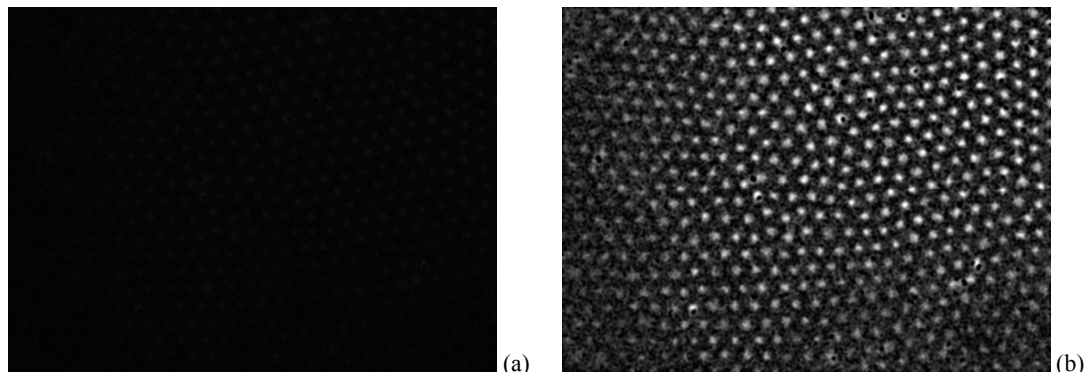


Fig. 5. (a) Fluorescent images before hybridizing with target miRNAs. (b) Fluorescent images after hybridizing with target miRNAs, where each bright spot corresponds to a cone with intensity highest at cone tip.

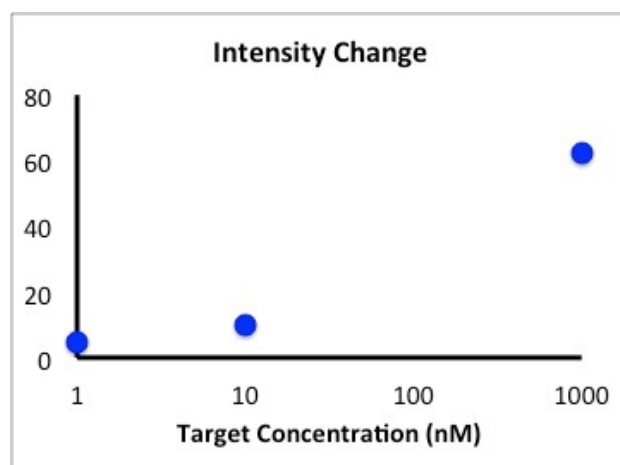


Fig. 6 Fluorescent intensity change for different concentration of miroRNAs.

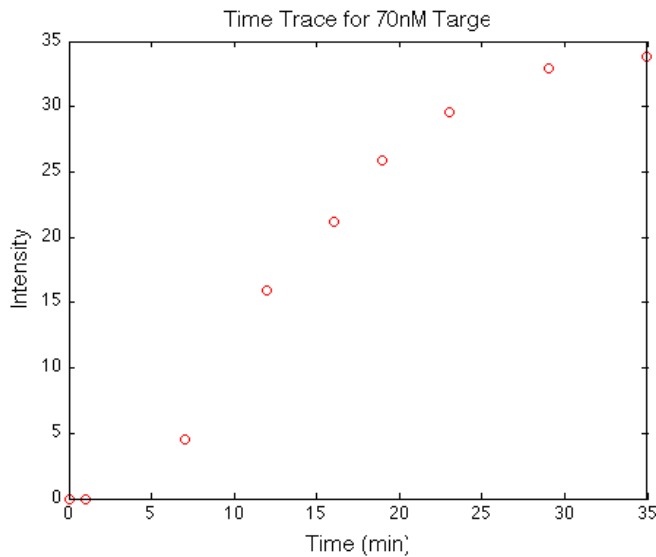


Fig. 6. Time response of fluorescent intensity change after adding target miRNAs.

-
- 1 Sonkoly, E. and Pivarcsi, A., "Advances in microRNAs: implications for immunity and inflammatory diseases", *J. Cell. Mol. Med.*, 13, 24-38 (2009).
- 2 Bakker, E. and Qin, Y., "Electrochemical sensors.", *Anal. Chem.*, 78, 3965-3984(2006).
- 3 Umezawa Y, Aoki H, "Ion channel sensors based on artificial receptors." *Anal. Chem.* 76: 321-326. (2004).
- 4 Wang Y, Plouraboue F and Chang H-C, "Broadband converging plasmon resonance at a conical nanotip.", *Opt Express*, 21 6609-6617 (2013).
- 5 Issa N. A. and Guckenberger R., "Optical nanofocusing on tapered metallic waveguides," *Plasmonics* 2, 31–37 (2007).
- 6 Lu X., Rycenga M., Skrabalak S., Wiley B., and Xia Y., "Chemical synthesis of novel plasmonic nanoparticles," *Annu. Rev. Phys. Chem.* 60, 167–192 (2009).
- 7 Deiss F and Sojic N and White D and Stoddart P, "Nanostructured optical fibre arrays for high-density biochemical sensing and remote imaging", 396:53–71(2010).